The Astrophysical Journal, 724:1542–1550, 2010 December 1 doi:10.1088/0004-637X/724/2/1542

GENERATION OF ELECTRIC CURRENTS IN THE CHROMOSPHERE VIA NEUTRAL–ION DRAG

V. Krasnoselskikh[1,2], G. Vekstein[3], H. S. Hudson[2,4], S. D. Bale[2], and W. P. Abbett[2]
[1] LPC2E, CNRS-University of Orléans, 3A Avenue de la Recherche Scientifique, 45071 Orléans Cedex 2, France
[2] Space Sciences Laboratory, University of California at Berkeley, CA 94720, USA
[3] School of Physics and Astronomy, The University of Manchester, Alan Turing Building, Manchester M13 9PL, UK
Received 2010 March 10; accepted 2010 September 27; published 2010 November 12

ABSTRACT

We consider the generation of electric currents in the solar chromosphere where the ionization level is typically low. We show that ambient electrons become magnetized even for weak magnetic fields (30 G); that is, their gyrofrequency becomes larger than the collision frequency while ion motions continue to be dominated by ion–neutral collisions. Under such conditions, ions are dragged by neutrals, and the magnetic field acts as if it is frozen-in to the dynamics of the neutral gas. However, magnetized electrons drift under the action of the electric and magnetic fields induced in the reference frame of ions moving with the neutral gas. We find that this relative motion of electrons and ions results in the generation of quite intense electric currents. The dissipation of these currents leads to resistive electron heating and efficient gas ionization. Ionization by electron–neutral impact does not alter the dynamics of the heavy particles; thus, the gas turbulent motions continue even when the plasma becomes fully ionized, and resistive dissipation continues to heat electrons and ions. This heating process is so efficient that it can result in typical temperature increases with altitude as large as 0.1–0.3 eV km^{-1}. We conclude that this process can play a major role in the heating of the chromosphere and corona.

Key words: Sun: chromosphere – Sun: photosphere

1. INTRODUCTION

The detailed physical mechanism of coronal heating is not yet well understood. A number of fundamental questions remain that challenge theoretical descriptions and the interpretation of observational data (see, e.g., Klimchuk 2006 or Walsh & Ireland 2003 for recent reviews). In addition, the heating of the chromosphere requires much more energy, and this related process is equally difficult to understand.

Parker (1988) proposed the idea that the solar corona could be heated by the episodic dissipation of energy at many small-scale tangential discontinuities arising spontaneously in the coronal magnetic field, as it becomes braided and twisted by random photospheric footpoint motions. These events—sudden changes of the magnetic field topology—hypothetically result in plasma heating and the acceleration of nonthermal particles. Parker invented a special name for these elementary energy release events, *nanoflares*. The inspiration for this was the discovery of the hard X-ray *microflares* by Lin et al. (1984); the energy of one nanoflare was to be roughly 10^{-9} times the energy of a major flare, and thus orders of magnitude weaker than even the microflares. Parker's idea stimulated intensive searches for any observational signatures of nanoflares (Cargill 1994; Sakamoto et al. 2008; Vekstein 2009) and their possible contribution to the overall energy budget of the solar corona (Klimchuk 2006).

Microflares were first detected in hard X-rays in a balloon experiment by Lin et al. (1984). The subsequent development of new instrumentation allowed the multi-wave satellite and ground-based high-resolution observations of smaller-scale (about a thousand kilometers or even smaller) and lower energy phenomena. Soft X-ray imaging revealed abundant microflares in active regions (Shimizu et al. 1994), and *RHESSI* observations found that virtually all of a sample of some 25,000 hard X-ray microflares occurred in active regions. Krucker et al. (1997) found flare-like brightenings in areas of the quiet Sun, and observations at EUV wavelengths (e.g., the "blinkers" of Harrison 1997) reveal bursting activity above the magnetic network borders. Similar phenomena that form small X-ray jets at the limb were reported by Koutchmy et al. (1997). From these and other EUV observations (Berghmans et al. 1998; Benz & Krucker 1998), if not the hard X-rays, we conclude that Parker's idea of episodic heating of the apparently steady quiet corona should not be discarded, even though no convincing evidence for the required steepening (Hudson 1991) of the energy distribution function has yet been presented.

However, the idea of coronal heating via tangential discontinuities that arise spontaneously (nanoflares) does not address two important questions. Namely, where does the excess magnetic energy come from, and what was its original source? Parker's analysis considered ideal MHD statistical equilibria that contain multiple discontinuities. Later Rappazzo et al. (2008) showed that a large-scale MHD energy source perturbed by slow motions on its boundary, supposed to be induced from the photosphere, results in the generation of a Poynting flux. This drives an anisotropic turbulent cascade dominated by magnetic energy. The result looks similar to Parker's tangling of magnetic field lines but the small-scale current sheets (which replace the tangential discontinuities) are continuously formed and dissipated. In this modification of the initial scenario the current sheets are the result of the turbulent cascade. The initial energy reservoir in such a view is contained in large-scale magnetic field structures.

Here, we discuss another possibility: the direct generation of relatively small-scale electric currents by neutral gas motions. Clearly, a huge energy reservoir exists in the form of turbulent motion of neutral gas at and beneath the photosphere, supported by the underlying convection zone. It is widely accepted that this energy can be partially transformed into the excess magnetic energy in the chromosphere and corona. However, there is no quantitative model that describes the physical mechanism of such energy transfer. The development of a model that describes the energy transfer from quasi-neutral gas motions

[4] Also at University of Glasgow, Glasgow G12 8QQ, UK.

to the magnetic field in a step-by-step manner inevitably raises questions about the spatial and temporal scales at which such a transfer can occur and about its location. Recent observations provide strong indications that the energy reservoir is indeed the dynamic turbulent photosphere, and that the energy transfer from the turbulent gas motions to various kinds of trapped and transient magnetic field oscillations takes place at the chromospheric level.

Analysis of the high-resolution spatial (∼150 km at the Sun) and temporal (few seconds) data obtained by the Solar Optical Telescope (SOT) aboard *Hinode* (De Pontieu et al. 2007) revealed that the chromosphere is dominated by a multitude of thin (∼200 km wide), dynamic, jetlike "type II" spicules. They are ejected upward with characteristic velocities of 20–150 km s^{-1} and reach heights of 2000–10000 km before disappearing from the chromospheric passband (in this case, the H line of Ca II). The type II spicules have quite short lifetimes of 10–300 s (according to the authors, most of them last less than 100 s) and many of them undergo substantial transverse displacements of the order of 500–1000 km. Moreover, the large-scale long-living spicules display oscillatory motions in the direction perpendicular to their own axes. Since the spicule structure can be taken to outline the direction of the magnetic field, this led the authors to the conclusion that the observed motions indicate Alfvénic oscillations.

Furthermore, the spatio-temporal variations of the chromosphere have always revealed the greatest complexity, and prominences also consist of numerous threadlike features with strong and mixed flows along these threads (Lin et al. 2005). Observations with SOT have provided an exceedingly variable and dynamic picture of these flows and field structures (Okamoto et al. 2009). The SOT chromospheric data are in the H line (Ca II), showing plasma at roughly 2×10^4 K. The movie presented by Okamoto et al (available on the *Hinode* Web site http://solarb.msfc.nasa.gov/) shows ubiquitous continuous motions along the prominence thread lines. The oscillatory motions observed might be interpreted in terms of propagating or standing Alfvén waves on the magnetic field lines that presumably compose the prominence. The typical transverse spatial scale of threads was found to be of the order of 600 km, with a characteristic length of the order of several megameters. The characteristic temporal scale was found to vary from 100 to several hundred seconds.

SOT observations near the limb led to the discovery of another small-scale dynamic phenomenon in the chromosphere: tiny chromospheric "anemone jets," named for the similar X-ray features (Shibata et al. 2007). They also resemble larger-scale features well known in Hα data and called surges or sprays, which often occur near sunspots and in association with flares or other transient activity (e.g., Rust 1968). All of these observations can be considered as indications of the generation of small-scale perturbations and oscillations of the magnetic field in the chromosphere, where the degree of ionization is still relatively small.

2. THE COUPLING PROBLEM

In spite of greatly improved observational data, the physics of chromospheric and coronal heating is not yet well understood. While the underlying mechanism must be associated with the magnetic field, the details of how efficiently the energy of convective motion is transformed into magnetic energy in the solar atmosphere is an open question. The importance of this process should not be understated. It is relevant not only to coronal heating and the acceleration of the solar wind, but also to the formation of the initial spectrum of wave turbulence introduced into the solar wind.

We propose a mechanism to generate electric currents that can be viewed as Alfvén or magnetosonic waves that result from strong ion–neutral drag. We assume that photospheric motions are turbulent, and consist of both compressional and rotational flows with energies exceeding that which is necessary to drive the observed oscillations of suspended threads or jets in the chromosphere. The question then becomes how these oscillations can be transported from the photosphere to the chromosphere, and how the flow of neutrals is transferred into the motion of charged particles and, ultimately, into the generation of electric current.

There are two physical processes that are necessary to convert the energy of the neutral gas motion into the magnetic field oscillations. Photospheric motions of charged particles are dominated by frequent electron–neutral and ion–neutral collisions, so that ions and electrons tend to follow the neutral gas motion with zero net electric current.

Since density falls off rapidly with height in the solar chromosphere, the electron collision frequency with neutrals and ions decreases to the point where it becomes smaller than the electron gyrofrequency. However, the ion–neutral collision frequency at this height still remains substantially larger than the ion gyrofrequency, since ion–neutral and electron–neutral collision rates are not substantially different (see, e.g., De Pontieu et al. 2001). Therefore, the motions of ions and electrons differ. Electrons tend to move along the magnetic field lines and drift due to $\mathbf{E} \times \mathbf{B}$ in the transverse direction, while the ions continue to move together with the neutrals. This difference results in the generation of electric currents.

To view this situation from a different perspective, if ions move together with neutrals (due to the strong drag) with some angle to the background magnetic field, an inductive electric field $\mathbf{v} \times \mathbf{B}$ appears in the reference frame of the plasma. This induced electric field inevitably generates electric currents that can be calculated using the plasma conductivity tensor. When electrons and ions are both demagnetized, this tensor reduces to the simple scalar conductivity, and the resulting current is very small. When electrons become magnetized, the motions of electrons and ions become decoupled, and the efficiency of the current generation is substantially higher.

Thus, we conclude that there is an efficient chromospheric dynamo operating in the layer between the level of electron magnetization and the height where either the degree of ionization becomes high (comparable with unity) or where the ions become magnetized. Forced oscillating currents are generated most effectively when the inductive electric field has characteristic frequencies and wavelengths close to the eigenmodes of the system, i.e., the MHD waves in the magnetized weakly ionized plasma. At higher altitudes, where ions are also magnetized, the motion of ions and electrons can still differ. However, under these conditions, both components will mainly move along the magnetic field lines and perform drift motions across the field. Thus, the current is directed mainly along the magnetic field lines, while in the intermediate region it can be generated in an arbitrary direction.

In summary, understanding how currents are generated by the turbulent motions of neutral gas in the photosphere can be broken down into two steps. First, we must understand how the energy and vorticity of photospheric motions are transported upward to the level where electron and ion motions become

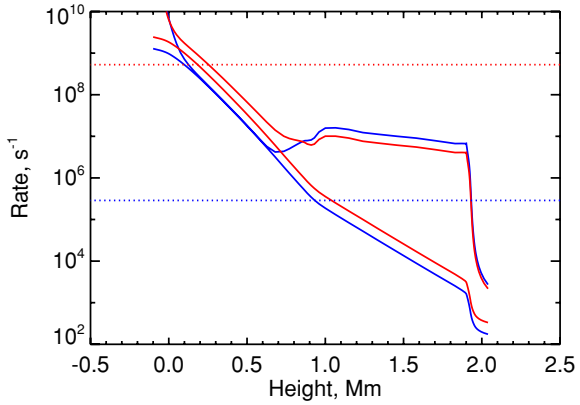

Figure 1. Collision frequencies in the quiet-Sun model of Fontenla et al. (2009). Blue (red) curves represent proton (electron) collision frequencies, with the lower lines showing neutral rates only (e.g., De Pontieu et al. 2001); the dotted horizontal lines show the gyrofrequencies (ions and electrons) for an assumed field strength of 30 G.

decoupled. Second, we must derive a self-consistent system of equations that describe the inductive electric field and the resulting deformation of the background magnetic field. Once we obtain the electric field and estimates of current density, we can then determine the efficiency of electron heating due to collisions and can investigate the efficacy of other possible heating mechanisms.

3. ATMOSPHERIC MODELS

We appeal to standard semi-empirical model atmospheres for approximate values of the physical parameters of the plasma in the photosphere and chromosphere. Fontenla et al. (2009) provide a recent series of eight such models representing features such as the quiet Sun, faculae, and sunspots. Such models are based on macroscopic radiative transport theory and are adjusted to recreate solar spectroscopic observations. They do not represent the dynamics, nor the plasma physics, since computer technology thus far allows at best only an MHD approach to the physics (e.g., Steiner 2007). Figure 1 compares collision frequencies from the Fontenla et al. (2009) quiet-Sun model (Model 1001) with the gyrofrequencies of electrons and ions. For this model we assume a constant magnetic field of 30 G (e.g., Harvey et al. 2007; Lites et al. 2008).

The Fontenla models cover a range of physical features in the solar atmosphere, and were originally intended for irradiance modeling. Here, we use these models as a guide to set a range of parameters that are reasonably consistent—in this limited theoretical framework—with solar structure. Figure 2 shows the location of the chromospheric dynamo layer for the full range of models. Electrons become magnetized, for all models, essentially throughout the solar atmosphere. Thus the chromospheric dynamo layer begins close to the photosphere and extends high into the chromosphere. This is true for all of the Fontenla models, ranging from sunspot umbra to bright facula, for which the transition-region pressures range from 0.2 to about 2.0 dyn cm^{-2}. Note that in such models, substantial hydrogen ionization does not take place below the transition region between chromospheric and coronal temperatures.

We emphasize that these models do not have any plasma physics in them as such, and only serve as references at the order-of-magnitude scale. Indeed, the mechanism discussed in this paper would point to areas in which models of the solar atmosphere can be greatly improved.

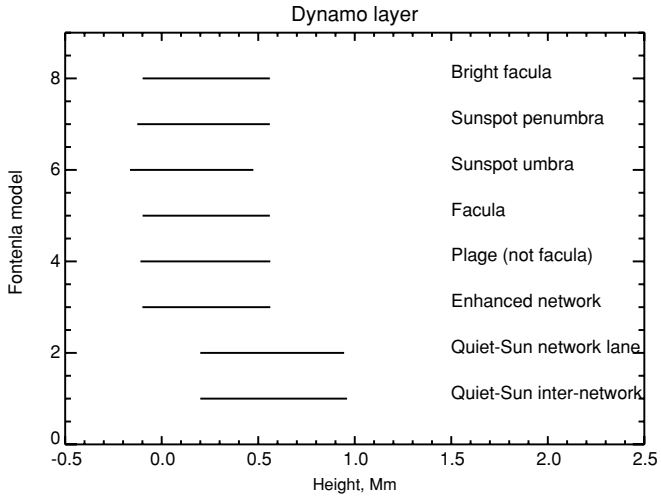

Figure 2. Chromospheric dynamo layers for the various solar features modeled by Fontenla et al. (2009). The field strengths assumed are 30 G for the quiet Sun (the lower two models) and 1500 G for the others.

4. ENERGY TRANSFER FROM THE PHOTOSPHERE TO THE CHROMOSPHERE

We first consider the physics of mass, momentum, and energy transport in the lower chromosphere. In order to formulate a mathematical description of the problem we need to take into account physical conditions between the photosphere and lower chromosphere, as described above.

We begin with an isothermal atmosphere, i.e., a gas having a constant sound speed and stratified by a uniform gravitational force acting in the negative z-direction, for which

$$\rho_0(z) = \rho_{\rm ph} \exp(-z/H). \quad (1)$$

Here, $\rho_{\rm ph}$ is the density at the level of the photosphere corresponding to $z = 0$, and H is the density scale height. The gas motions are described by the equation of continuity

$$\frac{\partial \rho}{\partial t} + \nabla \cdot \{(\rho_0 + \rho)\vec{v}\} = 0,$$

where the density is presented as the sum of hydrostatic equilibrium density and a perturbation (note that in hydrostatic equilibrium there are no flows).

By taking into account the equilibrium density dependence upon height this can be rewritten as

$$\frac{\partial}{\partial t}\left(\frac{\rho}{\rho_0}\right) + \frac{\partial v_x}{\partial x} + \frac{\partial v_y}{\partial y} + \left(\frac{\partial}{\partial z} - \frac{1}{H}\right) v_z = \frac{1}{H}\frac{\rho v_z}{\rho_0} - \nabla\left(\frac{\rho}{\rho_0}\vec{v}\right), \quad (2)$$

where we have separated the linear and nonlinear parts and put the latter on the right-hand side. The equation of motion

$$(\rho + \rho_0)\left(\frac{\partial \vec{v}}{\partial t} + (\vec{v}\nabla)\vec{v}\right) = -\nabla P - (\rho + \rho_0) G\hat{z}$$

takes the form

$$\frac{\partial \vec{v}}{\partial t} + \nabla\left(\frac{P}{\rho_0}\right) - \hat{z}\frac{1}{H}\left(\frac{P}{\rho_0}\right) + \left(\frac{\rho}{\rho_0}\right) G\hat{z} = -(v\nabla)v - \frac{\rho}{\rho_0}\left(\frac{\partial v}{\partial t} + (v\nabla)v\right). \quad (3)$$

We shall also use the equation of state taken in the simplified form of the equation for adiabatic motion,

$$\frac{dP}{dt} = \frac{\gamma P_{ph}}{\rho_{ph}} \frac{d}{dt}(\rho + \rho_0).$$

This is

$$\frac{dP}{dt} = C_S^2 \frac{d}{dt}(\rho + \rho_0).$$

It also can be rewritten for perturbations as

$$\frac{\partial}{\partial t}\left(\frac{P}{\rho_0}\right) - C_S^2 \frac{\partial}{\partial t}\left(\frac{\rho}{\rho_0}\right) + \frac{\gamma - 1}{\gamma}\frac{C_S^2}{H} v_z = C_S^2 \left[(\vec{v}\,\nabla)\frac{\rho}{\rho_0} - \frac{v_z}{H}\left(\frac{\rho}{\rho_0}\right)\right] - (\vec{v}\,\nabla)\left(\frac{P}{\rho_0}\right) + \frac{v_z}{H}\left(\frac{P}{\rho_0}\right). \quad (4)$$

Our objective here is the analysis of propagation of the photospheric perturbations upward into the chromosphere, and for this purpose we analyze the characteristics of linear perturbations. To obtain the linear wave mode dependences, we determine the eigenmodes of the linearized system:

$$\frac{\partial}{\partial t}\frac{\rho}{\rho_0} + \nabla \cdot \vec{v} - \frac{1}{H} v_z = 0 \Rightarrow \frac{\partial}{\partial t}\frac{\rho}{\rho_0} = -\nabla \cdot \vec{v} + \frac{1}{H} v_z, \quad (5)$$

$$\frac{\partial \vec{v}}{\partial t} + \nabla\left(\frac{P}{\rho_0}\right) - \hat{z}\frac{1}{H}\left(\frac{P}{\rho_0}\right) + \left(\frac{\rho}{\rho_0}\right) G\hat{z} = 0, \quad (6)$$

and

$$\frac{\partial}{\partial t}\left(\frac{P}{\rho_0}\right) + C_S^2 \nabla \cdot \vec{v} - \frac{1}{\gamma}\frac{C_S^2}{H} v_z = 0. \quad (7)$$

We choose standard solutions of the form

$$P, \rho, v \sim \exp i(\omega t - k_x x - k_y y - k_z z),$$

and analyze the dispersion relations that determine the dependences of the frequency ω upon components of the wave vector $\vec{k}$. But our problem is formulated as a boundary-value problem where we assume the perturbations and their time dependences to be prescribed at the boundary $z = 0$. We want to describe the evolution of perturbations with height z. In this case, the very same equations should be used to find out the dependence of the component k_z of the k-vector upon the frequency ω and other components k_x, k_y. Substituting dependences defined above into the linearized equations one can obtain the dispersion equation in the form

$$[\omega^2 - iKg]\left\{\omega^2 - C_S^2\left[(k^2 + K^2) + \frac{iK}{H}\frac{\gamma - 1}{\gamma}\right)\right]\right\} - iGC_S^2(k^2 + K^2)\left(K + \frac{i}{H}\frac{\gamma - 1}{\gamma}\right) = 0,$$

where $C_S^2 = \gamma G H$, $k^2 = k_x^2 + k_y^2$, $K = k_z - \frac{i}{H}$, and

$$k_z = \frac{i}{2H} \pm \sqrt{\frac{\omega^4 - \omega^2 C_S^2\left(k^2 + \frac{1}{4H^2}\right) + (\gamma - 1)k^2 g^2}{\omega^2 C_S^2}}.$$

This analysis demonstrates that a wide class of perturbations satisfying the condition

$$\omega^4 - \omega^2 C_S^2\left(k^2 + \frac{1}{4H^2}\right) + (\gamma - 1)k^2 G^2 > 0$$

increase with height, and the characteristic growth rate is

$$\Gamma = \mathrm{Im}(k_z) = \frac{1}{2H}.$$

This phenomenon, the "effective growth" of the perturbations with altitude in a hydrostatic gas equilibrium with exponentially decreasing density, is well known in the terrestrial atmosphere. It plays an important role in the propagation of infrasonic perturbations induced by explosions in the atmosphere (e.g., Klostermeyer 1969a, 1969b). The same physical phenomena play important roles in the solar photosphere and chromosphere and have been the subject of many observational, theoretical, and simulation studies. At low frequencies, acoustic gravity waves (purely hydrodynamic) play a role (e.g., Straus et al. 2008, 2009), and at high frequencies MHD modes (e.g., Hollweg 1986). The simulations (e.g., Stein & Nordlund 1998) can include essential physics such as optically thick radiative transfer.

The results of the more realistic simulations highlight important features of neutral gas motion. For example, vorticity is primarily generated due to baroclinic forces, and tends to concentrate in tube-like structures whose widths are comparable to the numerical resolution. In addition, plasma heating depends on the formation of supersonic flows and shock-like structures. If shocks form systematically, they could well be an important factor in the physics of coronal heating. However, according to Stein & Nordlund (1998), shocks are indeed observed at the edges of intergranular lanes, but are a rare occurrence. At any one time, supersonic flow occurs in only 3%–4% of the surface area.

The role of acoustic gravity waves has also been intensively studied experimentally. Recently new experimental studies combining the SOT/NFI and SOT/SP instruments on *Hinode* and the Michelson Doppler Imager (MDI) on *SOHO*, with the aid of three-dimensional computer simulations, were performed by Straus et al. (2009). The authors came to the conclusion that the gravity waves are the dominant phenomenon in the quiet middle/upper photosphere and that they transport sufficiently more mechanical energy than the high-frequency (>5 mHz) acoustic waves. In addition, they conclude that the acoustic gravity wave flux is 3–5 times larger than the upper-limit estimate of Fossum & Carlsson (2005). These observations together with the numerical models allow us to consider acoustic gravity waves as one of the most important sources from which energy may be transformed to the magnetic field, and then to heat via the action of electric currents.

We note that the absolute magnitude of the density perturbation actually decreases with height, but it drops more slowly than the background density. This results in the growth of the relative density perturbation, written as ρ/ρ_0 in our notation. On the other hand, the *velocity* perturbations really grow exponentially. An important issue here is the characteristic vertical scale of this growth. Taking the gas temperature to be 5000 K we find

$$H = \frac{k_B T}{MG} = 140 \text{ km}.$$

This linear analysis includes only the effect of the growth of the velocity and relative density perturbations with the altitude; hence, the perturbation scales do not vary with altitude. Of course, there are a wide range of phenomena, such as vortical flows, that are not accounted for in this formalism.

For example, the vortex radius can decrease with altitude. Indeed, assuming conservation of angular momentum, the increase of the velocity should result in the shrinking of the transverse diameter of the vortex. This effect is relevant for Rossby vortices in a multi-layer atmosphere and it is in good agreement with the observation of Stein & Nordlund (1998) that the vorticity concentrates in small-scale tubes.

5. MAGNETIC PERTURBATIONS PRODUCED BY THE TURBULENT MOTIONS OF THE NEUTRAL GAS

Turbulent convective fluid motions at the photospheric level extend upward into the lower chromosphere. The latter is a weakly ionized plasma with a typical temperature of 6000–7000 K, neutral hydrogen density $n_H \sim 10^{12}$–10^{14} cm^{-3}, and electron density $n_e \sim 10^{10}$–10^{11} cm^{-3}. Under these conditions, the frequency of the ion–neutral collisions is as high as $\nu_{\rm in} \approx 10^7$–$10^9$ s^{-1} which, as will be confirmed below, produces quite a strong drag effect resulting in the bulk velocity of ions, V_i, closely matching that of the neutral gas, V_n. Then the magnitude of the generated electric current $\vec{j} = n_e e(\vec{V_i} - \vec{V_e}) \approx n_e e(\vec{V_n} - \vec{V_e})$ is determined by the electron bulk velocity V_e. The latter is governed by the equation of motion for the electrons:

$$m_e \frac{d\vec{V_e}}{dt} = -e\{\vec{E} + [\vec{V_e} \times \vec{B}]\} - (\nu_{en} + \nu_{ei}) m_e (\vec{V_e} - \vec{V_n}), \quad (8)$$

where $\nu_{en} \approx 5 \times 10^8$–$10^{10}$ s^{-1} is the frequency of electron–neutral collisions, the major source of the electron drag. Here, ν_{ei} is the electron–ion collision frequency.

Ions are supposed to be dragged by neutrals; thus the velocity of electrons can be expressed as

$$\vec{V_e} = \vec{V_n} - \frac{\vec{j}}{en}.$$

The physical processes we describe occur in a parameter range corresponding to the transition in electron motions from unmagnetized, collision-dominated, to magnetized, when initially $|\omega_{Be}| < (\nu_{en}+\nu_{ei})$, and then with the growth of altitude $|\omega_{Be}|$ becomes larger than $(\nu_{en}+\nu_{ei})$. We consider hereafter slow motions $\omega \ll (\nu_{en} + \nu_{ei})$, $|\omega_{Be}|$ similar to those we described in the previous paragraph. In this case, one can neglect the electron inertia on the left-hand side of Equation (8). It can then be simplified to obtain

$$-e\left\{\vec{E} + [\vec{V_n} \times \vec{B}] - \frac{1}{ne}[\vec{j} \times \vec{B}]\right\} + (\nu_{en} + \nu_{ei}) m_e \frac{\vec{j}}{ne} = 0. \quad (9)$$

Taking the curl and replacing $\nabla \times B$ via

$$\frac{\partial \vec{B}}{\partial t} = -\nabla \times \vec{E}$$

one can obtain the final equation

$$\frac{\partial \vec{B}}{\partial t} = \nabla \times [\vec{V_n} \times \vec{B}] - \frac{1}{e\mu_0} \nabla \times \frac{1}{n} [\nabla \times \vec{B} \times \vec{B}] - \frac{(\nu_{en} + \nu_{ei}) m_e}{e^2 \mu_0} \nabla \times \frac{\nabla \times \vec{B}}{n}, \quad (10)$$

where $\vec{j}$ is replaced by

$$\vec{j} = \frac{1}{\mu_0} \nabla \times \vec{B}. \quad (11)$$

Equation (10) and the system of Equations (2)–(4) together make up a closed system describing an interaction of neutral gas perturbations with the ionized electron component that can result in generation of electric currents. We neglect hereafter the influence of electron motions on neutral gas motions by assuming that the degree of ionization is low.

In what follows, it is assumed that the chromospheric magnetic field can be represented as

$$\vec{B} = \vec{B_0} + \vec{b},$$

where $\vec{B_0}$ is a background field, which for the sake of simplicity is assumed here to be just a uniform field, while **b** is a relatively small field deformation caused by a prescribed flow of neutral gas with velocity $\vec{V_n}$ and frequency ω.

Then the linearized (with respect to **b**) version of Equation (10) takes the form

$$\vec{b} + i d_e^2 \frac{|\omega_{Be}|}{\omega} (\vec{h} \cdot \nabla) \nabla \times \vec{b} - d_e^2 \left(1 + i \frac{\nu_{en}}{\omega}\right) \nabla^2 \vec{b} = i \frac{B_0}{\omega} \{(\vec{h} \cdot \nabla) \vec{V_n} - \vec{h} (\nabla \cdot \vec{V_n})\}, \quad (12)$$

where **h** is the unit vector along the background magnetic field and $d_e = c/\omega_p e$ is the skin depth.

Let us now estimate the relative roles of the different terms on the left-hand side of Equation (12). For $n_e = 10^{11}$ cm^{-3} the electron plasma frequency $\omega_{pe} = 10^{10}$ s^{-1}, which yields $d_e \approx 3$ cm. The typical frequency of the neutral gas flows under consideration is $\omega \approx (10^{-2}$–$10^{-3})$ s^{-1} and their length scale is $L \sim 10^2$–10^3 km. For $B_0 \approx 100$ G the electron gyrofrequency $\omega_{Be} = 2 \times 10^9$ s^{-1}, while the characteristic electron–neutral collision frequency $\nu_{en} \sim (10^8$–$10^9)$s^{-1}. Therefore, the ratio of the second and third terms compared to the first can be considered small. Thus, Equation (12) can be reduced to

$$\vec{b} \approx i \frac{B_0}{\omega} \{(\vec{h} \cdot \nabla) \vec{V_n} - \vec{h} (\nabla \cdot \vec{V_n})\}, \quad (13)$$

which means that in the lower chromosphere the magnetic field is effectively frozen into the neutral-gas flow.

This describes the magnetic field generation due to the motions of conductive fluid neglecting small-scale effects scaling as the electron inertial length, and assuming the motions to be slow: $\omega \ll \Omega_e$. Let us now verify that the assumption made above, namely that the bulk velocity of the ions, $\vec{V_i}$, is so close to that of the neutrals, $\vec{V_n}$, that the electric current can be written as $\vec{j} = n_e e(\vec{V_n} - \vec{V_e})$. It can be easily found from expression (13) that

$$\vec{j} = \frac{1}{\mu_0} \nabla \times \vec{b} = i \frac{B_0}{\mu_0 \omega} \nabla \times \{(\vec{h} \cdot \nabla) \vec{V_n} - \vec{h} (\nabla \cdot \vec{V_n})\} \approx i \frac{B_0}{\mu_0 \omega} (\vec{h} \cdot \nabla) \nabla \times \vec{V_n}.$$

To evaluate the difference between the ion and neutral velocities let us consider the equation of motion for ions:

$$M_i \frac{d\vec{V_i}}{dt} = e\{\vec{E} + [\vec{V_i} \times \vec{B}]\} - M_i \nu_{\rm in} (\vec{V_i} - \vec{V_n}). \quad (14)$$

As can be seen from Equation (14), the sought-after velocity deviation $\Delta\vec{V_i} = (\vec{V_i} - \vec{V_n})$ is such that the ion–neutral drag

balances the other forces exerted upon the ions. A simple estimate shows that the net electromagnetic force is the dominant one there, and Equation (14) yields

$$M_i \nu_{\rm in} \overrightarrow{\Delta V_i} \approx e\{\overrightarrow{E} + [\overrightarrow{V_n} \times \overrightarrow{B}]\} \sim \frac{1}{n}[\overrightarrow{j} \times \overrightarrow{B}] + \frac{m_e}{en}\nu_{en}\overrightarrow{j}.$$

It follows then from Equation (14) that

$$\overrightarrow{\Delta V_i} \approx \frac{e \mid \{\overrightarrow{E} + [\overrightarrow{V_n} \times \overrightarrow{B}]\} \mid}{M_i \nu_{\rm in}} \sim \frac{\Omega_i}{\nu_{\rm in}} \frac{\mid \overrightarrow{j} \mid}{ne} \tag{15}$$

and

$$\overrightarrow{\Delta V_i} \sim \delta v_e \frac{\omega_{Bi}}{\nu_{\rm in}} < \delta v_e,$$

where δv_e is the velocity of current-carrying electrons, and ions are assumed to be demagnetized.

On the other hand, by using Equation (13), the electric current can be estimated as

$$j \sim \frac{b}{\mu_0 L} \sim \frac{B_0 V_n}{\mu_0 \omega H L}.$$

The velocity of the current-carrying electrons is

$$\delta v_e \sim \frac{j}{ne} \sim \frac{eB_0 V_n}{\mu_0 m \omega H L} \frac{m}{ne^2} \sim \frac{\omega_{Be}}{\omega} \frac{d_e^2}{HL} V_n < V_n. \tag{16}$$

It is seen now from Equations (15) and (16) that, indeed, $\delta V_i \ll V_n$ and $\delta V_i < \delta v_e$.

A simple estimate of the currents generated at different altitudes and for different values of the magnetic field can be obtained by assuming the neutral gas motions to be rotational. In this case, the characteristic velocity in the vortex V_n of characteristic spatial scale L rotating with the characteristic frequency ω can be evaluated as follows:

$$V_n \sim \omega L.$$

Thus, the characteristic magnetic field perturbation is

$$\delta B \sim B_0 \frac{L}{H},$$

and consequently the current density is

$$j \sim \frac{\delta B}{\mu_0 L} \sim \frac{B_0}{\mu_0 H}.$$

One can see that the magnetic field perturbations can become quite large; the current densities for magnetic fields of the order of 100 G can become as great as

$$j \sim \frac{B_0}{\mu_0 H} \sim 10^{-2}\text{–}10^{-1} \frac{A}{m^2}.$$

It is worth noting that this mechanism is dependent upon the velocity shear. An interesting feature of this process is the very high efficiency of the field generation around the boundaries of the neighboring vortices, where the characteristic shear of the velocity of the gas motions is large. In this case, the characteristic velocity shear is

$$\frac{V_n}{L} \gg \omega;$$

thus, smaller-scale magnetic field structures can be generated quite efficiently and magnetic fields generated and current densities can become tens or hundreds of times higher than the estimate above.

6. ELECTRON AND ION RESISTIVE HEATING

To evaluate the electron heating efficiency one should find the induced electric fields parallel and perpendicular to the magnetic field. This can be done in a straightforward way by making use of the component of the equation of motion for electrons along the magnetic field (Equation (8)):

$$m_e \frac{dV_{e\|}}{dt} = -eE_\| - \frac{\nu_{en} m_e}{ne} j_\|;$$

in the lowest-order approximation, one should take into account that the frequency ω of wave motions is much smaller than the electron–neutral collision frequency. This leads to the resistivity along the magnetic field to be classically collisional, where the dominant effect is due to electron–neutral collisions:

$$\begin{aligned} E_\| &= -\frac{\nu_{en} m_e}{ne^2} j_\| = -\frac{\nu_{en}}{\varepsilon_0 \omega_p^2} j_\| \\ &= -\frac{i\nu_{en}}{\mu_0 \varepsilon_0 \omega_p^2} \frac{B_0}{\omega} (\overrightarrow{h} \cdot \nabla \times \{(\overrightarrow{h} \cdot \nabla)\overrightarrow{V_n} - \overrightarrow{h}(\nabla \cdot \overrightarrow{V_n})\}) \\ &\sim \nu_{en} \frac{d^2}{L} \delta B. \end{aligned}$$

To evaluate the parallel electric field one should take into account that the electron–neutral collision frequency varies with height from $\nu_{\rm en} \sim 5 \times 10^8$ to 10^{10} s^{-1} and the plasma frequency varies in turn from 10^{10} to 10^{11}. Taking the characteristic current densities obtained above we find electric fields in the range

$$E_\| \approx (10^{-2}\text{–}10^{-1})\ \text{Vm}^{-1},$$

with the electron heating written (Braginskii 1965) as

$$\frac{3}{2} N_e \frac{d_e T_e}{dt} + p_e \nabla \cdot \overrightarrow{V_e} = -\nabla \cdot \overrightarrow{q_e} + Q_e. \tag{17}$$

Here, p_e is the electron pressure, and the electron heating Q_e is determined by two "friction forces," one due to the relative velocity between electrons and ions/neutrals ($\overrightarrow{R_{ei}}, \overrightarrow{R_{en}}$) and another due to the electron temperature gradient $\overrightarrow{R_T}$:

$$Q_e = (\overrightarrow{R_{ei}}, \overrightarrow{V_e} - \overrightarrow{V_i}) + (\overrightarrow{R_{en}}, \overrightarrow{V_e} - \overrightarrow{V_n}) + (\overrightarrow{R_T}, \overrightarrow{V_e} - \overrightarrow{V_n}),$$

with

$$\overrightarrow{R_{ei}} = -\nu_{ei} m_e N_e \{0.5(V_{e\|} - V_{i\|})\overrightarrow{h} + (\overrightarrow{V_{e\perp}} - \overrightarrow{V_{i\perp}})\},$$

$$\overrightarrow{R_{en}} = -\nu_{en} m_e N_e \{0.5(V_{e\|} - V_{n\|})\overrightarrow{h} + (\overrightarrow{V_{e\perp}} - \overrightarrow{V_{n\perp}})\},$$

and

$$\overrightarrow{R_T} = -0.7 N_e (\overrightarrow{h}, \nabla) T_e - \frac{3}{2} N_e \frac{\nu}{\Omega_e} [\overrightarrow{h}, \nabla T_e].$$

As a result

$$\begin{aligned} Q_e = &-\frac{(\nu_{ei} + \nu_{en}) m_e N_e}{N_e^2 e^2} \left\{ 0.5 j_\|^2 + j_\perp^2 \right. \\ &\left. + \frac{0.7 N_e^2 e}{\mu_0} (\overrightarrow{h} \cdot \nabla \times \overrightarrow{B})(\overrightarrow{h}, \nabla) T_e \right\}; \end{aligned} \tag{18}$$

here we neglect the difference between the ion and neutral velocities. The last term in the equation of energy balance to be kept describes the heat flux that is written as

$$\vec{q_e} = \vec{q_{ue}} + \vec{q_{Te}},$$

$$\vec{q_{ue}} = 0.7 N_e T_e (V_{e\parallel} - V_{n\parallel}) + \frac{3}{2} N_e T_e \frac{\nu}{\Omega_e} [\vec{h}, \vec{V_{e\perp}} - \vec{V_{i\perp}}],$$

and

$$\vec{q_{Te}} = -3.16 \frac{N_e T_e}{m_e(\nu_{en} + \nu_{ei})} \nabla_\parallel T_e - 4.66 \frac{N_e T_e (\nu_{en} + \nu_{ei})}{m_e \Omega_e^2} \nabla_\perp T_e - \frac{5}{2} \frac{N_e T_e}{m_e \Omega_e} [\vec{h}, \nabla_\perp T_e].$$

We shall begin by evaluating the energy supply provided by resistive dissipation that is determined by the first two terms on the right-hand side of the equation of energy balance. The volumetric heating power of the electrons can be estimated as

$$\frac{3}{2} n k_B \frac{dT_e}{dt} \sim j_\parallel E_\parallel \sim \frac{\nu_{en}}{\mu_0} \frac{d^2}{L^2} \delta B^2 \sim (10^{-4} \text{ to } 10^{-3}) \text{W m}^{-3}.$$

In a thermal equilibrium when the macroscopic flow evacuates the power supplied by collisional resistive dissipation, one can estimate the temperature variation with altitude as

$$\frac{dT_e}{dt} = V_{ez} \frac{\partial T_e}{\partial z}, \frac{\partial T_e}{\partial z} \sim \frac{j_\parallel E_\parallel}{\frac{3}{2} n k_B V_{ez}},$$

where V_{ez} is the characteristic macroscopic vertical velocity of electron (plasma) motion that can be evaluated to be of the order of the sound velocity. Then

$$\frac{\partial T_e}{\partial z} \sim \frac{j_\parallel E_\parallel}{\frac{3}{2} n k_B V_S} \sim (0.01\text{–}0.1) \text{ V km}^{-1}.$$

It is easy to see that the collisional heating of the electrons becomes rather efficient. Another possible evaluation of the temperature variation with altitude can be obtained by assuming a stationary static thermal equilibrium. Under such conditions the power supply will be balanced by the divergence of the heat flux in Equation (17), which can be estimated as

$$\nabla \cdot \vec{q_e} \approx \frac{\partial}{\partial z} \kappa_z^e \frac{\partial T_e}{\partial z},$$

where κ_z is the electron thermal conductivity in the parallel direction. For our conditions, when electron–neutral conditions are dominant in the parallel direction,

$$\kappa_z^e \approx \gamma \frac{n_e T_e}{m_e \nu_{en}},$$

where γ is a coefficient of order unity (according to Braginskii 1965) for electron–ion collisions; when ions are singly ionized it is equal to ~3.8. This leads to the following estimate of the characteristic heat loss rate:

$$\nabla \cdot \vec{q_e} \approx \frac{\partial}{\partial z} \gamma \frac{k_B n_e T_e}{m_e \nu_{en}} \frac{\partial k_B T_e}{\partial z} \sim \frac{k_B^2 n_e T_e^2}{m_e \nu_{en} L_T^2},$$

where (T_e/L_T) is the characteristic variation of temperature with altitude. Under the physical conditions of the chromosphere this will lead to

$$\left(\frac{T_e}{L_T}\right) \sim \left(\frac{j_\parallel E_\parallel m_e \nu_{en}}{k_B^2 n_e}\right)^{1/2} \sim 0.1\text{–}0.3 \text{ eV km}^{-1}.$$

Taking into account an exponential decrease of the plasma density one can find that it can heat plasma to the hydrogen ionization energy (13.6 eV) on a characteristic distance of the order of a few hundred kilometers. It should be noted, however, that the thermal conductivity increases with the temperature and this can result in some flattening of the temperature profile.

Another important physical effect is related to the ion heating due to the perpendicular electric fields. It is known that the major component of the current along the electric field perpendicular to the magnetic (the Pedersen current) can be carried by ions. This can lead to the more efficient heating of ions than of electrons. To evaluate the Pedersen current we must estimate the ion velocity deviation from the velocity of neutrals in the direction of the electric field, as was already done in the previous paragraph:

$$\vec{\Delta V_i} \approx \frac{e \mid \{\vec{E} + [\vec{V_n} \times \vec{B}]\} \mid}{M_i \nu_{\text{in}}} \sim \frac{1}{M_i \nu_{\text{in}} n} [\vec{j} \times \vec{B}] \sim \frac{j B_0}{n M_i \nu_{\text{in}}}.$$

It follows then that

$$(n_e \vec{\Delta V_i} \cdot \{\vec{E} + [\vec{V_n} \times \vec{B}]\}) \sim \frac{j^2 B_0^2}{n M_i \nu_{\text{in}}} \sim \frac{M_i}{m_e} \frac{\Omega_i^2}{\nu_{\text{in}}} \frac{d^2}{L^2} \delta B^2.$$

Ion heating due to the perpendicular electric field component can be evaluated as

$$\frac{dT_i}{dt} \sim (\vec{j_{\perp i}} \cdot \{\vec{E} + [\vec{V_n} \times \vec{B}]\}) \sim \frac{M_i}{m_e} \frac{\Omega_i^2}{\nu_{en} \nu_{\text{in}}} \frac{dT_e}{dt}.$$

This estimate shows that the ion collisional heating can be several times smaller than, or comparable to, the electron heating.

7. DISCUSSION

The current generation mechanism that we propose here is strongly dependent upon four basic parameters: the velocity of the turbulent gas motions, the background magnetic field, the characteristic frequency of the spectrum of turbulent motions of the gas, and the characteristic spatial scale of velocity shear. The physical process of the generation of electric currents and magnetic fields is actually nothing other than the well-known turbulent-dynamo mechanism operating as a result of the freezing of the magnetic field into the flow of the neutral gas.

The altitudes where this mechanism will operate are strongly dependent upon the local magnetic field strength: the stronger the field, the lower the altitude of electron magnetization. The efficiency of the electric current generation is proportional to the magnitude of the velocity shear. The characteristic spatial scales are proportional to the characteristic scales of this velocity shear, i.e., the flow vorticity. It is interesting to note that, in this formalism, magnetic fields and currents can be generated by both compressible and incompressible motions (see the first and second terms in Equation (13)). Compressive motion tends to amplify or weaken the background magnetic field, while the rotational component effectively generates the

perpendicular or helical components of the field. This means that compressional motions tend to generate transverse currents, while non-compressional motions can generate field-aligned currents as well.

Since density tends to decrease exponentially with height in the chromosphere, the characteristic velocities of chromospheric flows can increase by a factor of 10 or more over their photospheric values. This gives rise to an estimate of the characteristic magnetic field generated by such motions readily becoming comparable to or even larger than the background field. Their relative magnitude is determined by the ratio of the characteristic velocity of neutral motions at the altitude of electron magnetization to the characteristic parameter ωH. One can see that for characteristic frequencies of the order of 10^{-2}–10^{-3} s^{-1}, and characteristic heights of the order of 140 km, the field generation becomes quite efficient already for velocities of the order of ten to several tens of km s^{-1}. The helical magnetic field component can become larger than the background field. A similar estimate shows that amplification/weakening of the background magnetic field component can be evaluated to be of the order of

$$\frac{b}{B_0} \sim \frac{\delta n}{n}.$$

Under such conditions, we show that the electron heating can become rather efficient due to the collisional resistive dissipation of the electric current. These processes take place in the regions where the magnetic field vorticity increases.

It is worth noting that the efficiency of the electron and ion heating can become substantially more important than that due to the collisional resistive dissipation described above. The electric current and magnetic field generation we have discussed take place at the chromospheric footpoints of flux tubes that may extend into the corona. The direction of the generated field is determined by the characteristics of the gas velocity shear and can lead to the formation of magnetic field configurations that can become unstable, or can form new structures by interaction with neighboring fields with different orientations. The increase of the perpendicular component of the magnetic field can result in kink instability if this component satisfies the Kruskal–Shafranov condition

$$\frac{\delta B}{B} > \frac{l}{R}.$$

Here, l is the characteristic scale of the cross section of the tube and R is its characteristic length. Under such conditions the tube cannot keep its configuration intact; it will become unstable and then different kinds of perturbations will result in its reconfiguration. Other types of emerging configurations with magnetic field inversions will result in local reconnection. The detailed study of these effects lies beyond the scope of our paper and will be carried out elsewhere.

The result of the heating would be a rapid increase of the degree of ionization of the gas. It is worth remembering that our whole description is valid only when the degree of ionization is low. This rapid ionization process can lead, according to most radiative–convective models (e.g., Stein & Nordlund 1998), to an efficient decrease of the radiative cooling rate of the gas. Thus the generation of electric currents results not only in the plasma heating itself, but also causes a decrease of the cooling process that will then strengthen the effect of radiative heating. We cannot make any quantitative estimate of these effects, but they may be addressed in future simulations.

The coupling of acoustic-type waves and MHD waves can also be treated in the MHD approximation (e.g., Hollweg et al. 1982). The major difference in our approach here is that the neutral collisions reduce the feedback effect on the motion of the gas resulting from the newly generated magnetic field. This produces a more efficient transfer of energy from gas motions to current generation and magnetic field amplification.

It seems possible to incorporate certain aspects of this formalism into a system of conservation equations similar to those used in Abbett (2007). In that work, the resistive MHD equations were solved numerically within a computational domain that includes both a turbulent model convection zone and corona. We are currently updating this system of equations to incorporate additional physics, and are planning to perform a comparison between a standard resistive radiative-MHD model and our new results. We hope to report on the results of this study in the near future.

8. CONCLUSION

We have presented an analysis of the effect of electric current and associated magnetic field generation in a "chromospheric dynamo layer" where electrons become magnetized while ions remain collisionally coupled to the neutrals. We have shown that electric currents and magnetic fields can be generated very efficiently due to turbulent motions of the neutral gas. The efficiency of this physical process is proportional to the characteristic velocity shear of the gas turbulent motions and inversely proportional to their characteristic frequency. We also found that the magnetic fields thus generated can be comparable to or even larger than the background magnetic field for motions having characteristic scales of the order of several hundred kilometers and characteristic timescales of the order of several minutes. This can produce a substantial restructuring of magnetic field configurations and an opportunity to create multiple sites of reconnection. It also results in an efficient increase of collisional resistive heating of electrons and ions, and hence the rapid ionization of the gas, thus unstably altering its thermal equilibrium.

The authors are grateful to CNES for financial support in the frame of a CNES "Solar Orbiter Research grant" and to SSL for the financial support of the visit of V.K. to the University of California at Berkeley. H.S.H. thanks NASA for support under NAG5-12878. V.K. acknowledges very useful discussions with M. Ruderman, B. De Pontieu, O. Podladchikova, and X. Valliers. The authors also thank the referee, whose comments helped in improving the article.

REFERENCES

Abbett, W. P. 2007, ApJ, 665, 1469
Benz, A. O., & Krucker, S. 1998, Sol. Phys., 182, 349
Berghmans, D., Clette, F., & Moses, D. 1998, A&A, 336, 1039
Braginskii, S. I. 1965, Rev. Plasma Phys., 1, 205
Cargill, P. J. 1994, ApJ, 422, 381
De Pontieu, B., Martens, P. C. H., & Hudson, H. S. 2001, ApJ, 558, 859
De Pontieu, B., et al. 2007, PASJ, 59, 655
Fontenla, J. M., Curdt, W., Haberreiter, M., Harder, J., & Tian, H. 2009, ApJ, 707, 482
Fossum, A., & Carlsson, M. 2005, Nature, 435, 919
Harrison, R. A. 1997, Sol. Phys., 175, 467
Harvey, J. W., Branston, D., Henney, C. J., Keller, C. U., & SOLIS and GONG Teams, 2007, ApJ, 659, L177
Hollweg, J. V. 1986, J. Geophys. Res., 91, 4111
Hollweg, J. V., Jackson, S., & Galloway, D. 1982, Sol. Phys., 75, 35

Hudson, H. S. 1991, Sol. Phys., 133, 357
Klimchuk, J. A. 2006, Sol. Phys., 234, 41
Klostermeyer, J. 1969a, J. Atmos. Terr. Phys., 31, 25
Klostermeyer, J. 1969b, Ann. Geophys., 25, 547
Koutchmy, S., Hara, H., Suematsu, Y., & Reardon, K. 1997, A&A, 320, L33
Krucker, S., Benz, A. O., Bastian, T. S., & Acton, L. W. 1997, ApJ, 488, 499
Lin, R. P., Schwartz, R. A., Kane, S. R., Pelling, R. M., & Hurley, K. C. 1984, ApJ, 283, 421
Lin, Y., Engvold, O., Rouppe van der Voort, L., Wiik, J. E., & Berger, T. E. 2005, Sol. Phys., 226, 239
Lites, B. W., et al. 2008, ApJ, 672, 1237
Okamoto, T. J., et al. 2009, ApJ, 697, 913
Parker, E. N. 1988, ApJ, 330, 474
Rappazzo, A. F., Velli, M., Einaudi, G., & Dahlburg, R. B. 2008, ApJ, 677, 1348
Rust, D. M. 1968, in IAU Symp. 35, Structure and Development of Solar Active Regions, ed. K. O. Kiepenheuer (Dordrecht: Reidel), 77
Sakamoto, Y., Tsuneta, S., & Vekstein, G. 2008, ApJ, 689, 1421
Shibata, K., et al. 2007, Science, 318, 1591
Shimizu, T., Tsuneta, S., Acton, L. W., Lemen, J. R., Ogawara, Y., & Uchida, Y. 1994, ApJ, 422, 906
Stein, R. F., & Nordlund, A. 1998, ApJ, 499, 914
Steiner, O. 2007, in AIP Conf. Ser. 919, Kodai School on Solar Physics, ed. S. S. Hasan & D. Banerjee (Melville, NY: AIP), 74
Straus, T., Fleck, B., Jefferies, S. M., Cauzzi, G., McIntosh, S. W., Reardon, K., Severino, G., & Steffen, M. 2008, ApJ, 681, L125
Straus, T., Fleck, B., Jefferies, S. M., McIntosh, S. W., Severino, G., Steffen, M., & Tarbell, T. D. 2009, in ASP Conf. Ser. 415, The Second Hinode Science Meeting: Beyond Discovery-Toward Understanding, ed. B. Lites, M. Cheung, T. Magara, J. Mariska, & K. Reeves (San Francisco, CA: ASP), 95
Vekstein, G. 2009, A&A, 499, L5
Walsh, R. W., & Ireland, J. 2003, A&AR, 12, 1